

BOND MECHANISMS OF NEAR SURFACE MOUNTED FRP BARS AND STRIPS FOR FLEXURAL STRENGTHENING OF CONCRETE STRUCTURES

Tarek Hassan
Post-Doctoral Fellow, Department of
Civil Engineering, North Carolina State
University, Campus Box 7533, Raleigh,
NC, USA 27695-7533

Sami Rizkalla
Distinguished Professor, Department of
Civil Engineering, North Carolina State
University, Campus Box 7533, Raleigh,
NC, USA 27695-7533

Abstract

Flexural strengthening of concrete structures and bridges with Fibre Reinforced Polymer (FRP) composites is an attractive alternative to traditional techniques. Externally bonded FRP sheets and strips have been widely accepted for strengthening civil infrastructure. In spite of the significant research being reported on their structural mechanism and performance, there are still heightened concerns regarding possible premature failure due to debonding, especially in zones of combined high flexural and shear stresses. Recently, considerable research has been directed to characterize the use of FRP bars and strips mounted in grooves at the tension zones.

This paper proposes two different analytical models to evaluate the bond characteristics of near surface mounted FRP bars and strips, respectively. The models are proposed to predict the interfacial shear stresses and the minimum anchorage length needed for the reinforcement. The proposed analytical models are validated by comparing the predicted values with test results as well as non-linear finite element modelling. Quantitative criteria governing debonding failure of near surface mounted FRP bars and strips are established.

INTRODUCTION

Bond of reinforcing FRP bars, strips and sheets to concrete is a critical factor that controls the structural performance of concrete members strengthened with FRP. Up-to-date, limited research has been reported on the bond behavior of near surface mounted (NSM) FRP reinforcement. Lack of experimental data, design tools and analytical models addressing the bond characteristics of various FRP strengthening techniques introduce serious obstacles towards an efficient use of these materials.

Near surface mounting technique becomes particularly attractive for flexural strengthening in the negative moment regions of slabs and girders, where externally bonded reinforcement could be subjected to severe damage due to mechanical and environmental conditions. The initial research work on NSM technique was reported by Blaschko (1999) using CFRP strips inserted into grooves cut at the surface of concrete specimens. The specimens were tested in a double shear configuration. Test results showed that strengthening using NSM CFRP strips has a greater anchoring capacity compared to externally bonded CFRP strips. De Lorenzis and Nanni (2001) investigated the structural performance of simply supported reinforced concrete beams strengthened with NSM GFRP and CFRP rods. Both flexural and shear strengthening were examined. Hassan and Rizkalla (2002) investigated the feasibility of using different strengthening techniques as well as different types of FRP for flexural strengthening of large-scale prestressed concrete specimens. The specimens represented typical prestressed concrete slab bridges. Test results showed that the use of NSM FRP bars is feasible and cost effective for strengthening concrete structures and bridges.

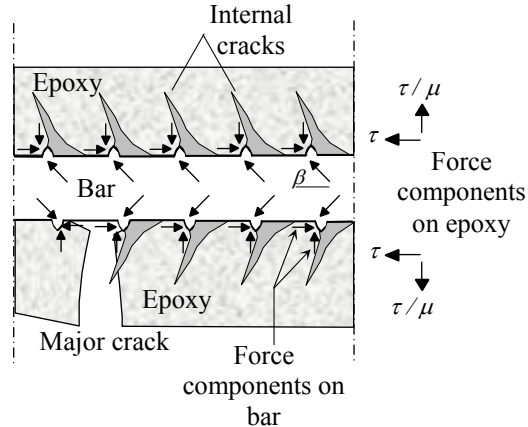
This paper presents design guidelines for an efficient use of NSM FRP bars and strips. Analytical models are proposed to fully characterize the behavior of concrete structures strengthened with NSM FRP bars and strips. The study offers quantitative information regarding debonding failures and emphasizes the influence of the configuration of the original steel reinforcement on the behavior. Design guidelines are provided to assist in establishing specifications on the use of NSM FRP reinforcement for strengthening concrete structures.

NSM FRP BARS

Transfer of stresses from a deformed NSM FRP rod to the concrete is mainly by mechanical interlocking of the lugs with the surrounding epoxy. The resultant force exerted by the lug on the epoxy is inclined at an angle β to the axis of the bar as shown in Fig. 1, where $1/\tan \beta$ is the coefficient of friction, μ , between the bar and the adhesive. The radial component of the resultant force creates zones of high tensile stresses at the FRP-epoxy interface as well as at the concrete-epoxy interface. Thick-walled cylinder theory was applied by many researchers to analyze the stresses in a concrete cylinder surrounding a single steel bar. Nevertheless, the same theory could not be applied for NSM FRP bars. Lack of confinement, uneven distribution of bond stresses and composite

interaction between concrete, epoxy and FRP materials complicate the analysis of NSM FRP bars and consequently, thick-walled cylinder theory is not valid in this case.

Fig. 1. Forces between a NSM FRP bar and adhesive



Finite element analysis was employed to provide in-depth understanding of the load transfer mechanism between NSM FRP bars and concrete. Fig. 2 shows the mesh dimensions used in modelling a portion of a concrete beam strengthened with a NSM FRP bar. The concrete and the epoxy were modelled using 8-node plain strain elements. Groove dimensions, bar location and properties of concrete and epoxy were set identical to the bond specimens tested by Rizkalla and Hassan, 2002. Radial pressure was applied at the bar location to simulate the bond stresses transferred from the bar to the surrounding epoxy. Typical principal tensile stress distribution is shown in Fig. 3.

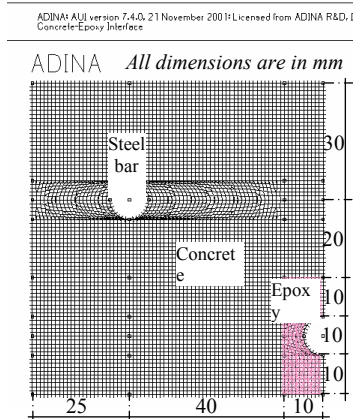


Fig. 2. Mesh dimension for a portion of a concrete beam strengthened with a NSM FRP bar

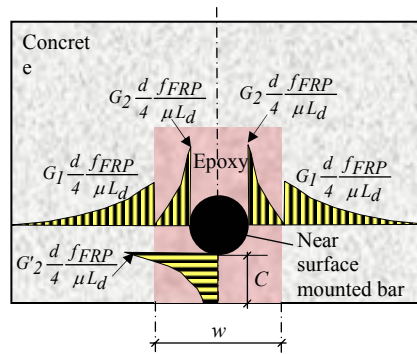


Fig. 3. Typical tensile stress distribution around NSM FRP bars

It should be noted that the elastic modulus of the adhesive is generally less than that of the concrete. Such a phenomenon results in a stress discontinuity at the concrete-epoxy interface as shown in Fig. 3. High tensile stresses are observed at the concrete-epoxy interface as well as at the FRP-epoxy interface. Two different types of debonding failures could occur for NSM FRP bars. The first mode of failure is due to splitting of the epoxy cover as a result of high tensile stresses at the FRP-epoxy interface, and is termed “epoxy split failure”. Increasing the thickness of the epoxy cover reduces the induced tensile stresses significantly. Furthermore, using adhesives of high tensile strength delays epoxy split failure. This type of debonding failure forms with longitudinal cracking through the epoxy cover (De Lorenzis and Nanni, 2002). The second mode of failure is due to cracking of the concrete surrounding the epoxy adhesive and is termed “concrete split failure”. This mode of failure will take place when the tensile stresses at the concrete-epoxy interface reaches the tensile strength of the concrete. Widening the groove minimizes the induced tensile stresses at the concrete-epoxy interface and increases the debonding loads of NSM bars. Concrete split failure was the governing mode of failure for the bond specimens tested by Rizkalla and Hassan, 2002. Large epoxy cover and high tensile strength of the epoxy adhesive provided high resistance to epoxy split failure and shifted the failure to occur at the concrete-epoxy interface.

Measurements of bar strains along the embedment length of NSM FRP bars shows linear strain distribution at high load levels. Therefore, the tangential bond stress, τ , is constant and can be expressed as:

$$\tau = \frac{d f_{FRP}}{4 L_d} \quad (2)$$

where d is the diameter of the bar, and L_d is the embedment length needed to develop a stress of f_{FRP} in the NSM bar. If the coefficient of friction between the bar and the epoxy is μ , the radial stresses, σ_{radial} , can be expressed as:

$$\sigma_{radial} = \frac{\tau}{\mu} = \frac{d f_{FRP}}{4 \mu L_d} \quad (3)$$

The tensile stresses at the concrete-epoxy interface, $\sigma_{con-epoxy}$, and at the FRP-epoxy interface, $\sigma_{FRP-epoxy}$, can be expressed in terms of the radial stress as follows:

$$\sigma_{con-epoxy} = G_1 \frac{d f_{FRP}}{4 \mu L_d} \quad (4)$$

$$\sigma_{FRP-epoxy} = G_2 \text{ or } G'_2 \left[\frac{d f_{FRP}}{4 \mu L_d} \right] \quad (5)$$

where G_1 , G_2 and G'_2 are coefficients determined from the finite element analysis based on a unit radial pressure applied at the bar location and using specified groove

dimensions, concrete and adhesive properties. The maximum tensile stresses at the FRP-epoxy interface, $\sigma_{FRP-epoxy}$, depends on the coefficients G_2 and G'_2 , whichever is greater as shown in Fig. 3. Equating the tensile strength of concrete to Eq. (4), the minimum embedment length needed for NSM FRP bars to prevent concrete split failure can be expressed as:

$$L_d = G_1 \frac{d f_{FRP}}{4 \mu f_{ct}} \quad (6)$$

Equating the tensile strength of the adhesive to Eq. (5), the minimum embedment length needed for NSM FRP bars to avoid epoxy split failure shall not be less than:

$$L_d = G_2 \text{ or } G'_2 \left[\frac{d f_{FRP}}{4 \mu f_{epoxy}} \right] \quad (7)$$

where f_{ct} and f_{epoxy} are the tensile strength of concrete and epoxy, respectively.

Increasing the ratio of the elastic modulus of the concrete to that of the adhesive, n , generates high tensile stresses at the concrete-epoxy interface and low tensile stresses at the FRP-epoxy interface. Practical values of the modular ratio, n , could vary between 5 and 40. This range covers various types of concrete and adhesives that are commonly used in concrete structures. Fig. 4 shows the proposed design chart for the development length of NSM FRP bars.

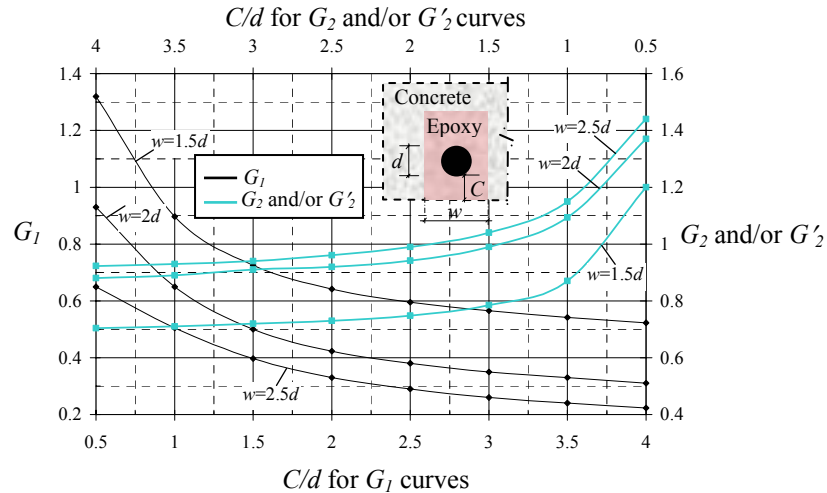


Fig. 4 Design chart for the development length of NSM FRP bars

To simulate the most critical conditions for design purposes, the coefficient G_1 was evaluated for a modular ratio of 40. The coefficients, G_2 and G'_2 were evaluated for a modular ratio 5 and the greater value was plotted in Fig. 4. The chart covers a wide range

of possible epoxy covers and accounts for three different groove sizes. Using the proposed design chart, the coefficients G_1 and the greater value of either G_2 or G'_2 could be evaluated for a given groove width, w , and using a specified clear cover to bar diameter ratio (C/d). The governing development length for NSM FRP bars could be predicted using the greater of Eqs. (6) and (7).

Verification of the Proposed Model

Test results showed that the coefficient of friction between CFRP bars and different epoxy adhesives has an average lower bound value of 0.33. Using a groove width equals to two times the diameter of the bar ($w=2d$) and a clear cover to bar diameter ratio of one ($C/d=1.0$), the coefficients G_1 and the greater of G_2 and G'_2 for the bond specimens tested by Rizkalla and Hassan, 2002 are 0.65 and 1.1, respectively. The diameter of the bar is 9.525 mm. The average tensile strength of the concrete and epoxy used in the bond specimens are 4.3 MPa and 48 MPa, respectively. Using Eqs. (6) and (7), the minimum embedment length needed to develop 40 percent of the ultimate strength of the bars, as measured by the experimental program, shall not be less than 834 mm, which coincides with the measured value of 800 mm.

Maximum Tensile Stresses in NSM FRP Bars (f_{FRP})

Rizkalla and Hassan, 2002 showed that the maximum tensile stress in NSM CFRP bars at the onset of debonding did not exceed 43% of the tensile strength of the bars regardless of the embedment length used. De Lorenzis and Nanni, 2002 reported a limiting tensile stress of 33% for NSM CFRP bars. It should be mentioned that the limiting tensile stress is highly dependent of the configuration of the internal steel reinforcement. Termination or damage of the internal steel reinforcement creates zones of high bond stress concentration and accelerates debonding failure for NSM FRP bars. Consequently, evaluation of the existing concrete structures and identifying the conditions as well as the configuration of the internal steel reinforcement is essential prior to strengthening using NSM FRP bars. The influence of various configurations of the bottom steel reinforcement on the behavior was investigated based on a non-linear finite element modelling. The analysis indicated that terminating 10 percent of the main bottom steel reinforcement allowed the CFRP bars to utilize 60% of its tensile strength prior to debonding. It should be noted that terminating 50% or more of the main bottom steel reinforcement had a negligible effect on the tensile stresses in the CFRP bars at the onset of debonding failure. In these cases, extremely high bond stresses were developed and the maximum induced tensile stresses in CFRP bars did not exceed 40 percent of the tensile strength of the bars, which coincided with the measured values by Rizkalla and Hassan, 2002. Increasing the area of the terminated and/or damaged steel reinforcement results in a proportional increase in the axial stiffness of the bars and consequently, high tensile stresses are developed in the bars. Equilibrium and compatibility provisions require full transmission of these tensile stresses in the terminated steel bars to neighbouring steel and FRP bars. Such a phenomenon results in a significant increase in

the bond stress and a corresponding decrease in the loads initiating debonding of the FRP bars.

Typical procedures to evaluate the development length of any configuration of NSM FRP bars can be summarized as follows:

- Determine the material characteristics of FRP bars, concrete and adhesive.
- Determine the coefficient of friction between the FRP bar and the bonding adhesive according to the ASTM G115-98 or based on information provided by the manufacturer.
- Select groove dimensions, thickness of the clear epoxy cover and use the proposed design chart, given in Fig. 4 to determine the coefficients G_1 and the greater of coefficients G_2 and/or G'_2 .
- Calculate the development length using the greater of Eq. (6) and Eq. (7).
- Reselect groove dimensions if necessary and repeat steps (c) to (e).

NSM FRP STRIPS

This section presents a closed-form analytical solution to predict the interfacial shear stresses for NSM FRP strips. The model is validated by comparing the predicted values with test results (Hassan and Rizkalla 2002). The proposed model is based on the combined shear-bending model for externally bonded FRP plates and is given in Fig. 5.

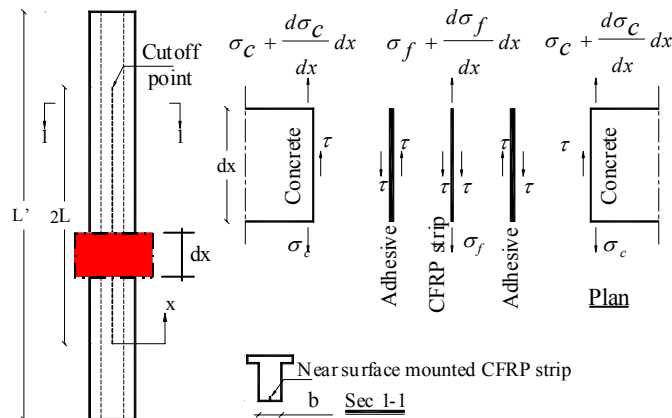


Fig. 5. Analytical model for NSM FRP strips

The model is modified to account for the double bonded area of NSM strips. The model accounts also for the continuous reduction in flexural stiffness due to cracking of the concrete. Debonding of NSM strips is assumed to occur as a result of high shear stress concentration at cutoff point. The derivation of the model is reported elsewhere

(Hassan and Rizkalla 2002). For simply supported beams subjected to a concentrated load, P , at midspan, the shear stress at the strip cutoff point, τ can be expressed in terms of the effective moment of inertia, I_{eff} , and the thickness of the CFRP strip, t_f , as follows:

$$\tau = \frac{t_f}{2} \left[\frac{n P l_o y}{2 I_{eff}} \omega + \frac{n P y}{2 I_{eff}} \right] \quad (8)$$

where,

$$\omega^2 = \frac{2 G_a}{t_a t_f E_f} \quad (9)$$

$$n = \frac{E_f}{E_c} \quad (10)$$

E_f is elastic modulus of the FRP strip, E_c is elastic modulus of concrete, G_a is the shear modulus of the adhesive, t_a is the thickness of the adhesive, l_o is the unbonded length of the strip; y is the distance from the strip to the neutral axis of the transformed section and I_{eff} is the effective moment of inertia of the transformed section. Debonding will occur when the shear stress reaches a maximum value, which depends on the concrete properties. Premature debonding of NSM CFRP strips is governed by the shear strength of the concrete. Other components of the system such as the adhesive and the CFRP strips have superior strength and adhesion properties compared to concrete. Knowing the compressive and tensile strength of concrete, the Mohr-Coulomb line, which is tangential to both Mohr's circles for pure tension and pure compression, can be represented and the maximum critical shear stress for the pure shear circle can be expressed as:

$$\tau_{max} = \frac{f'_c f_{ct}}{f'_c + f_{ct}} \quad (11)$$

where f'_c is the compressive strength of concrete after 28 days and f_{ct} is the splitting tensile strength of concrete. Equating the shear strength proposed in Eq. (11) to the shear stress given in Eq. (8), debonding loads for NSM CFRP strips can be determined for this specific loading case and embedment length. Other loading cases are reported in Hassan and Rizkalla, 2002. The development length is highly dependent on the dimensions of the strips, concrete properties, adhesive properties, internal steel reinforcement ratio, reinforcement configuration, type of loading, and groove width. The proposed model in Eqs. (8) and (11), can be used to estimate the development length of NSM strips of any configuration as follows:

a) Use the proposed Eqs. (8) and (11) to determine the debonding load of the strip for different embedment lengths as shown in Fig. 6. The resulting curve represents a failure envelope due to debonding of the strip at cutoff point.

- b) Use a cracked section analysis at sections of maximum induced normal stresses and determine the ultimate load required to rupture the strip as shown in Fig. 6.
- c) Determine the development length at the intersection of the line corresponding to flexural failure of the strip with the curve representing debonding failure at cutoff point.

The calculated development length will preclude brittle failure due to debonding of the strips and will ensure full composite action between the strip and concrete up to failure. The proposed approach compared very well with the experimental results reported by Hassan and Rizkalla, 2002. The predicted debonding loads underestimated the measured values by less than 6%

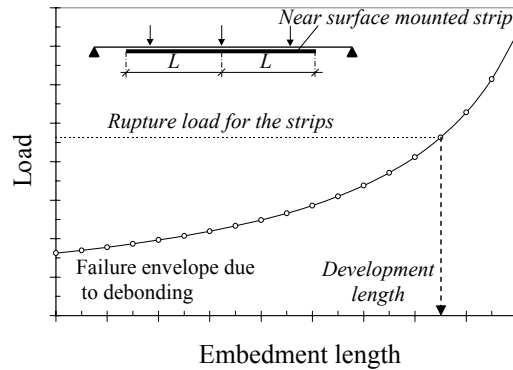


Fig. 6. General procedures to determine the development length of NSM strips

STRUCTURAL HEALTH MONITORING FOR INNOVATIVE FRP SYSTEMS

As the technology of near surface mounting emerges, the structural behavior of reinforced concrete structures strengthened with NSM FRP bars and/or strips needs to be continuously monitored. During the last decade, field experience has been gained in terms of the operational performance of Fibre Optic Bragg Gratings Sensors. The failure rate of some of these sensors is far less than conventional strain gauge sensors. Fibre optic sensors can be structurally integrated during the manufacturing process of FRP bars and strips used as NSM reinforcement. Fibre optic sensors also provide the opportunity to use modern telecommunication technologies to serve the long-term “health” monitoring of strengthened concrete structures and bridges.

CONCLUSIONS

Based on the findings of this investigation, the following conclusions can be drawn:

1. The efficiency of using CFRP bars as NSM reinforcement is controlled primarily by the bond characteristics of the bars as well as by the bond between the adhesive material and the concrete.
2. Two different types of debonding failures can occur for NSM FRP bars:
i- Epoxy split failure ii- concrete split failure.
3. The proposed design chart is adequate to determine the development length of NSM FRP bars accurately. The chart is easy to use and provides excellent correlation to experimental results.
4. Increasing the groove width and/or using high strength concrete, increases the resistance to concrete split failure. Using high strength adhesives and/or increasing the epoxy cover layer delays epoxy split failure for NSM FRP bars.
5. The proposed analytical model for NSM FRP strips is capable of predicting the interfacial shear stress distribution, ultimate load carrying capacity and mode of failure of concrete beams strengthened with NSM FRP strips.
6. The proposed failure criterion for debonding of NSM CFRP strips provided sufficient evidence and confidence in predicting debonding loads.

REFERENCES

1. Blaschko, M., and Zilch, K. (1999). "Rehabilitation of concrete structures with strips glued into slits." *Proc., 12th Int. Conf. on Composite Materials*, Paris, CD-Rom.
2. De Lorenzis L., and Nanni, A. (2001). "Shear strengthening of reinforced concrete beams with near-surface mounted fibre reinforced polymer rods." *ACI Struct. J.*, 98 (1) 60-68.
3. Hassan, T., and Rizkalla, S. (2002). "Flexural strengthening of prestressed bridge slabs with FRP systems." *PCI J.*, 47 (1) 76-93.
4. Hassan, T., and Rizkalla, S. (2002). "Investigation of bond in concrete structures strengthened with near surface mounted CFRP strips." *ASCE J. of Comp. for Const.*, *Accepted for publication*.
5. De Lorenzis L. and Nanni, A., (2002) "A bond between near-surface mounted FRP rods and concrete in structural strengthening", *ACI Struct. J.*, 99 (2) 123-132.
6. Rizkalla, S., and Hassan T., (2002) "Effectiveness of FRP techniques for strengthening concrete bridges" *J. of the Int. Ass. for Bridge and Struct. Engng. IABSE*, 12 (1) May 2002.